Vertical ozone simulation in the middle atmosphere

C.A. VAROTSOS

Department of Applied Physics, University of Athens,

33 Ippokratous Str., Athens 106 80, Greece

Abstract

Simulations of the ozone mixing ratio over midlatitudes of the northern hemisphere, as a function of the height and time, based on multiple data sets from satellites are presented.

1. Introduction

Since detailed knowledge of the global distribution of ozone is important for studies of atmospheric circulation, dynamic processes, radiation balance and the photochemistry of the atmosphere, numerous models have been developed to summarise the features of the latitudinal and seasonal variations of the ozone content.(Varotsos and Cracknell,1993; Varotsos et al, 1994) These models, however, were based on various portions of the available measurements obtained from the ground and from balloons, rockets and satellites. For instance, models relating the vertical distribution of ozone to total ozone amount based on approximately 7000 balloonsondes and a number of rocketsondes, were generated as a "first guess" for the Nimbus-4 Backscattered Ultraviolet (BUV) ozone experiment retrievals of total ozone and its vertical structure and for the Nimbus-7 SBUV / TOMS total ozone retrievals (Mateer et al. 1980). Klenk et al. (1984) developed a model of ozone vertical structure based on Nimbus-4 BUV observations and on balloon data. This model was used as a "first guess" for vertical structure retrievals from the Nimbus-7 Solar Backscattered Ultraviolet (SBUV) ozone experiment.

It is thus of great importance to know fairly well the features of the ozone sphere over the midlatitude areas of the northern hemisphere and to generate models of ozone vertical structure from this geographical region, based not just on data from one satellite, but on all the available multiple data sets from satellites. It is the main purpose of the present paper to propose simulations of the ozone mixing ratio over midlatitudes of the northern hemisphere, as a function of height (pressure) and time, based on multiple data sets from satellites.

2. Analysis method and results

The ozone data we have used for the purposes of the present study are from five satellite experiments (each covering a different height region): the Nimbus-7 Solar Backscattered Ultraviolet (SBUV), the Nimbus-7 Limb Infrared Monitor of the Stratosphere (LIMS), the Applications Explorer Mission-2 Stratospheric Aerosol and Gas Experiment (SAGE), the Solar Mesosphere Explorer UV Spectrophotometer (SME-UVS), and the Solar Mesosphere Explorer 1.27 μm Airglow (SME-IR). The very good absolute accuracy of the individual data sets allowed the data to be directly combined over the period 1978-1982 (Keating and Young, 1985).

We have selected the latitudes of 30°N, 40°N, and 50°N in order to investigate the vertical ozone profiles over Greece (extended from 35°N to 43°N). It is considered that the total ozone is not dependent on longitude. This assumption is safe due to the fact the longitudinal variations in total ozone amount are very small compared with the latitudinal ones.

Figure 1 shows the vertical distribution of the zonal mean ozone volume mixing ratio at 40°N for the months of the year, as it is derived from a best fit, using equation (1), and a combination of data from all the data sets mentioned above (solid line). The data have been analysed using the best fit to an equation of the form

$$\psi = D_1 (\alpha_1 x^2 + \alpha_2 x + \alpha_3) + D_2 (\alpha_4 x + \alpha_5) \qquad (1)$$

where ψ = ozone concentration in ppmv

and x = pressure level in hPa.

The values of D_1 and D_2 are either

$$D_1 = 1, \quad D_2 = 0 \qquad (2)$$

or

$$D_1 = 0, \quad D_2 = 1 \qquad (3)$$

depending on the value of x; in other words we use a linear relation for one range of x and a parabolic relation for the remainder of the range. Figure 1 also illustrates the best fit approximation (dashed line) applied on the vertical ozone data derived from the satellite observations. Table 1 provides the values of the coefficients in the regression equations and Table 2 the values of the corresponding regression coefficients for each of the three latitudes 30°N, 40°N and 50°N.

The seasons are considered as December, January, February and March for winter time, September, October and November for autumn time and April, May, June, July and August for summer time. We have also determined least squares fits, using

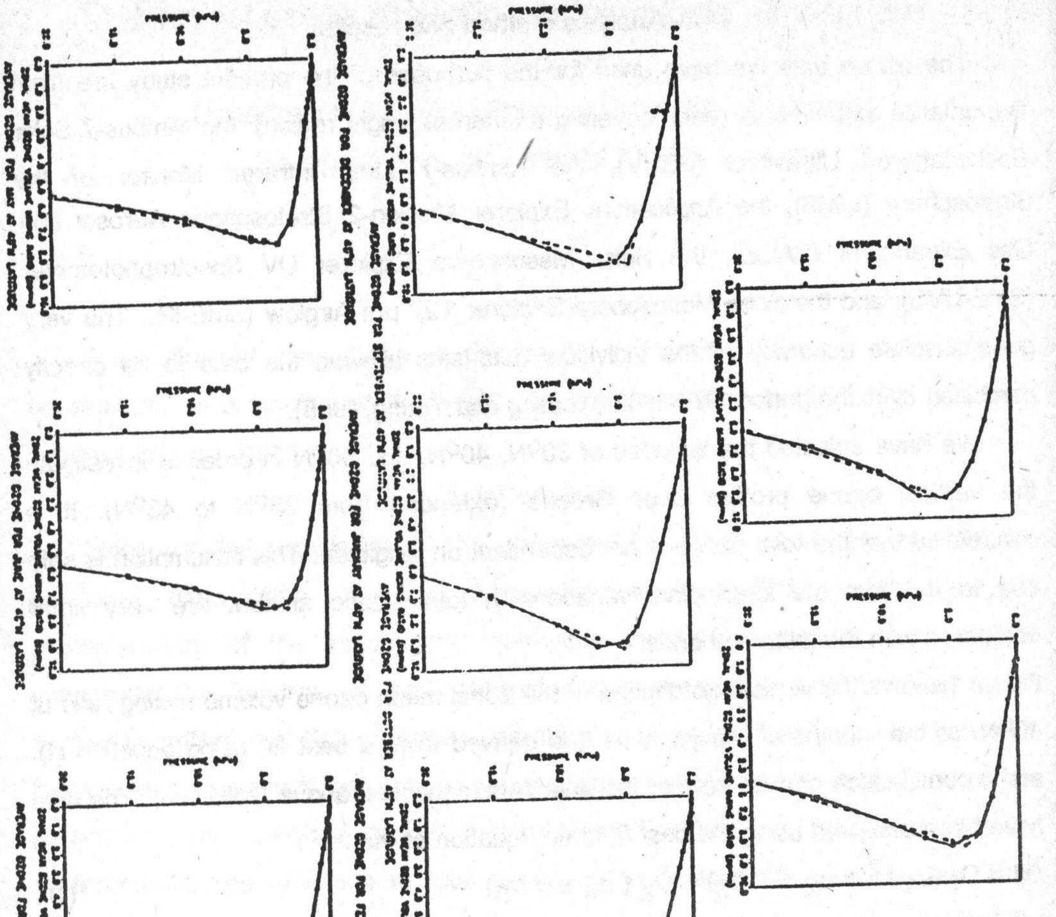

(a) (b) (c)

Figure 1: Profiles of the zonal mean ozone volume mixing ratio derived from multiple set of satellite data (solid line) at 30^{O}N. Best fit curve (dashed line) (a) For winter time (December, January, February, March) (b) For summer time (May, June, July, August) (c) For autumn time (September, October, November)

Table 1: Values of coefficients for best fits in the equations for the vertical ozone volume mixing ratio (ψ, in ppmv), versus pressure (x, in hPa), at 30°N, 40°N and 50°N, for monthly data.

Months	Latitude (°N)	Coefficients					
		a_1	a_2	a_3	a_4	a_5	x_l ∠1
January	30	-0.254	3.434	0.275	-0.134	8.584	2
	40	-0.424	3.908	0.291	-0.118	7.944	
	50	-0.604	4.204	0.300	-0.113	7.313	
February	30	-0.216	3.266	0.295	-0.151	9.140	2
	40	-0.210	3.593	0.278	-0.147	8.524	
	50	-0.434	4.139	0.254	-0.114	7.708	
March	30	-0.267	3.216	0.324	-0.168	9.816	3
	40	-0.280	3.427	0.296	-0.187	9.494	
	50	-0.382	3.802	0.253	-0.178	8.949	
April	30	-0.203	2.963	0.415	-0.142	9.743	3
	40	-0.164	2.902	0.399	-0.177	9.696	
	50	-0.163	2.938	0.340	-0.198	9.524	
May	30	-0.217	2.931	0.380	-0.133	9.757	3
	40	-0.176	2.780	0.390	-0.155	9.570	
	50	-0.146	2.656	0.374	-0.160	9.166	
June	30	-0.234	3.005	0.348	-0.211	10.875	4
	40	-0.191	2.776	0.382	-0.211	10.318	
	50	-0.203	2.670	0.376	-0.187	9.429	
July	30	-0.282	3.239	0.309	-0.210	10.912	4
	40	-0.246	3.010	0.331	-0.206	10.302	
	50	-0.194	2.717	0.341	-0.200	9.686	
August	30	-0.353	3.498	0.275	-0.205	10.693	4
	40	-0.355	3.417	0.271	-0.195	10.019	
	50	-0.326	3.205	0.268	-0.190	9.293	
September	30	-0.295	3.374	0.287	-0.232	11.157	4
	40	-0.342	3.487	0.259	-0.219	10.339	
	50	-0.396	3.630	0.215	-0.207	9.429	
October	30	-0.254	3.291	0.303	-0.187	10.142	3
	40	-0.393	3.784	0.260	-0.184	9.232	
	50	-0.606	4.438	0.195	-0.166	8.309	
November	30	-0.209	3.241	0.321	-0.125	8.753	2
	40	-0.168	3.611	0.307	-0.163	8.414	
	50	-0.326	4.191	0.267	-0.156	7.753	
December	30	-0.223	3.300	0.318	-0.129	8.466	2
	40	-0.191	3.594	0.335	-0.141	8.071	
	50	-0.352	4.048	0.325	-0.140	7.411	

$D_1 = 1, \quad D_2 = 0 \quad \text{if} \quad x < x_l \;, \quad D_1 = 0, \quad D_2 = 1 \quad \text{if} \quad x > x_l$

Table 2: Monthly regression coefficients (x^2-test) between the model and the fitted ozone values, at 30°N, 40°N and 50°N.

MONTH	REGRESSION COEFFICIENT		
	30°N	40°N	50°N
January	0.953	0.956	0.947
February	0.960	0.954	0.956
March	0.959	0.957	0.954
April	0.954	0.959	0.964
May	0.955	0.957	0.949
June	0.967	0.958	0.942
July	0.970	0.965	0.954
August	0.961	0.955	0.958
September	0.966	0.961	0.961
October	0.959	0.957	0.954
November	0.959	0.949	0.956
December	0.951	0.963	0.942

equation (1), to the seasonal average data and the values of the coefficients obtained are presented in table 3 and the corresponding regression coefficients are given in Table 4 for latitudes 30°N, 40°N and 50°N. Inspection of Figure 1, shows that: (a) the region of the transition from the linear-type approximation to the parabolic-type approximation (which is equivalently the region of the maximum ozone volume mixing ratio) is lower during summer-time and higher during winter-time, (b) in the stratosphere the ozone mixing ratio increases with height with a rate which is larger during summer-time comparing with winter-time, (c) in the mesosphere the ozone mixing ratio decreases with height with a rate which is larger during winter-time comparing with summer-time and (d) in the stratosphere the ozone mixing ratio decreases going from 30°N to 50°N at the same month and at the same pressure level.

Table 3: Values of coefficients for best fits in the equations for the vertical ozone mixing ratio (ψ, in ppmv), versus pressure level (x, in hPa) at 30°N, 40°N and 50°N, for seasonal average data.

Season	Coefficients						
	Latitude (°N)	α_1	α_2	α_3	α_4	α_5	x_l 1)
Winter	30	-0.224	3.307	0.302	-0.135	8.734	2
	40	-0.249	3.681	0.301	-0.143	8.242	
	50	-0.432	4.150	0.287	-0.131	7.547	
Autumn	30	-0.237	3.103	0.355	-0.157	9.866	3
	40	-0.254	3.224	0.336	-0.176	9.499	
	50	-0.324	3.460	0.290	-0.175	8.985	
Summer	30	-0.291	3.279	0.305	-0.215	10.911	4
	40	-0.283	3.171	0.311	-0.208	10.246	
	50	-0.279	3.054	0.301	-0.196	9.459	

1) $D_1 = 1, \quad D_2 = 0 \quad \text{if} \quad x<x_l$

$D_1 = 0, \quad D_2 = 1 \quad \text{if} \quad x>x_l$

Table 4: Seasonal regression coefficients (x^2-test) between the model and the fitted ozone values, at 30°N, 40°N and 50°N.

SEASON	REGRESSION COEFFICIENT		
	30°N	40°N	50°N
Winter	0.958	0.962	0.945
Autumn	0.960	0.952	0.950
Summer	0.965	0.958	0.951

The physical meaning of the linear best fit of the ozone volume mixing ratio versus pressure in the region 20-5 hPa and the parabolic fit in the region above the 5 hPa pressure level can be described as follows: The stratospheric ozone is produced by photodissociation of molecular oxygen (O_2 + hv → 2O) followed by a three-body recombination reaction (O + O_2 + M → O_3 + M). In the latter reaction M is a third molecule which is required to carry away the excess energy released in the reaction. On the other hand the stratospheric ozone is destroy by its recombination with atomic oxygen (O_3 + O → 2O_2). However, the latter reaction can be catalysed by a number of atmospheric species (OH, NO, NO_2, Cl, ClO). In the lower and middle stratosphere (20-5 hPa) the effect of nitrogen is the dominant ozone loss (WMO, 1985). Given that the amounts of the nitrogen species are linearly dependent on pressure at the lower and middle stratosphere (WMO, 1985) a linear dependence on pressure of the ozone mixing ratio is expected at this atmospheric region. In the upper stratosphere and the mesosphere (above 5 hPa) the destruction by hydrogen compounds dominates (WMO, 1985). Due to the fact that the concentration of hydrogen compounds increases parabolically with height, a parabolic decrease in the ozone amount is therefore expected.

Acknowledgements

Authors express their gratitude to Mr. N. Papanikolaou for the data analysis.

References

Keating, G. M., and D. F. Young, "Interim reference ozone models for the middle atmosphere", Middle Atmosphere Programme, Handbook for MAP, Vol. 16, 205-229, (1985).

Klenk, K. F., B. Monosmith, and P. K. Bhartia, Paper 7.6, Proc. Quad-rennial Ozone Symp., Halkidiki, Greece, (1984).

Mateer, C. L., J. J. DeLuisi, and C. C. Porco, "The short Umkehr method, part I: Standard ozone profiles for the use in the estimation of ozone profiles by the inversion of short Umkehr observations", NOAA Tech. Memo. ERL ARL-86, 20 pp., NOAA Air Resources Laboratories, Silver Spring, MD, (1980).

Stolarski, R. S., P. Bloomfield, R. D. McPeters, and J. R. Herman, "Total Ozone trends deduced from Nimbus 7 TOMS data", Geophysical Research Letters, 18, 6, 1015-1018, (1991).

Varotsos, C., A. P. Cracknell, "Ozone depletion over Greece as deduced from Nimbus-7 TOMS measurements", International Journal of Remote Sensing, 14, 2053-2059, (1993).

Varotsos, C., P. Kalabokas, and A. P. Cracknell, "Intercomparison of ozone models derived by remote and in situ sensing techniques with recent local measurements at middle latitudes", International Journal of Remote Sensing (in press), (1994).

WMO, "Atmospheric Ozone", Report No. 16, 648 pp., WMO, Geneva, (1985).